PCCP

Accepted Manuscript

This is an *Accepted Manuscript*, which has been through the Royal Society of Chemistry peer review process and has been accepted for publication.

Accepted Manuscripts are published online shortly after acceptance, before technical editing, formatting and proof reading. Using this free service, authors can make their results available to the community, in citable form, before we publish the edited article. We will replace this *Accepted Manuscript* with the edited and formatted *Advance Article* as soon as it is available.

You can find more information about *Accepted Manuscripts* in the Information for Authors.

Please note that technical editing may introduce minor changes to the text and/or graphics, which may alter content. The journal's standard Terms & Conditions and the Ethical guidelines still apply. In no event shall the Royal Society of Chemistry be held responsible for any errors or omissions in this *Accepted Manuscript* or any consequences arising from the use of any information it contains.

ROYAL SOCIETY OF CHEMISTRY

www.rsc.org/pccp

Journal Name

ARTICLE

Strategies for Modulation the Luminescent Properties of Pyronin Y Dye-Clay Films: Experimental and Theoretical Study

Received 00th January 20xx,
Accepted 00th January 20xx

DOI: 10.1039/x0xx00000x

www.rsc.org/

Nerea Epelde-Elezcano,[a] Virginia Martínez-Martínez,[a*] Eduardo Duque-Redondo,[a] Inés Temiño,[a] Hegoi Manzano [a*] and Iñigo López-Arbeloa [a]

The aggregation process, particularly type and extent, of pyronin Y (PY) laser dye intercalated into supported thin films of two different trioctahedral clays minerals, laponite (Lap) and saponite (Sap), at different dye loadings is studied: i) experimentally by means of electronic absorption and fluorescence spectroscopies and ii) theoretically by modeling the distribution of the dye into the interlayer space of these layered silicates. According to the results, H-type aggregates of the PY dye are favoured in Lap even at very low dye loading while a much lower molecular aggregation tendency in J-type geometry is found in Sap films. The aggregation state of PY in each clay mineral are likely attributed to the different strength of the electrostatic interactions between the dye and the layered silicate in the interlayer space due to their distinctive charge localization on the TOT clay layer (i.e. net negative charge in octahedral layers for Lap vs in tetrahedral layers for Sap), as well as the interlaminar water distribution in each clay mineral, although other factors such as their CEC and their particle size cannot be discarded . To reduce the huge aggregation processes of PY dye into Lap films, surfactant molecules (DDTAB) are co-adsorbed in the interlayer space of the clay. At an optimized surfactant concentration, the aggregation tendency of PY dye in Lap is considerably reduced improving enormously the fluorescent efficiency of the PY/Lap films. Finally, by means of the anisotropic response from the hybrid films to the plane of the polarized light, the orientation of the PY molecules respect to the normal axis of the clay layer is determined for all films (with and without surfactant) at different dye loadings.

INTRODUCTION

The interest in the development of multifunctional materials with optical properties has increased exponentially. Many benefits are gained by the combination of organic (guest) and inorganic (host) components since the host will provide a better thermal and chemical stability to the molecules embedded, to the guest molecules[1,2]. Indeed, many functional hybrid systems used as in solid-states tunable lasers[3] or photovoltaic cells[4] are based on encapsulation of photoactive molecules, i.e. organic dyes into different inorganic matrices[5]. Furthermore, the matrix could also induce a preferential orientation to the guest molecules obtaining a macroscopic ordered system, important for many optical devices such as frequency-doublers, dichroic filters and light waveguides[6,7]. In this sense, layered clay minerals are attractive host materials with well-organized 2D multilayer structure that can be easily obtained by elaborating supporting films[1,8]. Thus, by the intercalation of photoactive molecules in the interlayer space of clays could be achieved a preferential orientation with respect the clay film[9–20].

Clay minerals are the most used laminar systems as inorganic host because of their optical transparency and high absorption capacity by cationic exchange mechanism quantified by their respective cation exchange capacity (CEC).

The smectite-type clays with a cationic exchangeable capacity between 50-100 meq/100g present the best swelling capacity to accommodate a large amount of cationic or polar molecules[21]. Generally, smectite layers are formed by the condensation of tetrahedral SiO_2 (T) and octahedral Al_2O_3 or MgO (O) layers. The isomorphic substitution of tetrahedral Si^{4+} and/or octahedral Al^{3+} or Mg^{2+} cations by other cations produce the net negative charged layers that are compensated by exchangeable inorganic cations in the interlayer space. In this work, two different smectite clay minerals are used as inorganic host: laponite (Lap) with octahedral substitution and saponite (Sap) with tetrahedral substitution (Scheme1)[22].

[a] Departamento de Química Física, Universidad del País Vasco, UPV/EHU, Apartado 644, 48080 Bilbao, Spain. E-mail: virginia.martinez@ehu.eus and Hegoi.manzano@ehu.eus

Electronic Supplementary Information (ESI) available: Absorbance and fluorescence spectra of PY in different media and in Lap films with surfactants, density profile of the interlaminar spaces of PY/Lap and PY/Sap films and the evolution of the dichroic ratio and its relationship with the twisted δ angle for several systems. See DOI: 10.1039/x0xx00000x

This journal is © The Royal Society of Chemistry 20xx

Please do not adjust margins

Physical Chemistry Chemical Physics Accepted Manuscript

Scheme 1. Schematic representation of a layer of (A) laponite and (B) saponite. The SiO_2 and Al_2O_3 tetrahedra are represented in yellow and orange respectively, whereas the MgO and Li_2O octahedra are shown in blue and green respectively

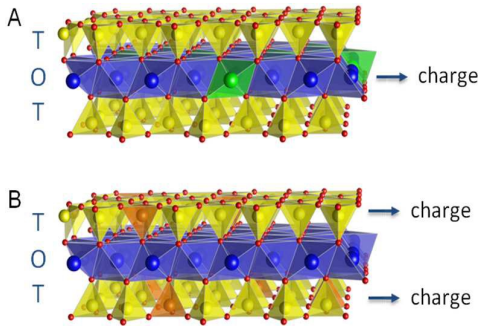

On the other hand, a xanthene dye, pyronin Y (PY), characterized for its bright pink color and high fluorescence quantum yield (ϕ_{fl}= 0.66 in ethanol), is chosen as guest to be adsorbed in clay mineral interlayers by ion exchange mechanism. However, xanthene-like dyes usually have a large molecular aggregation tendency in concentrated solutions or in adsorbed-state [15,23–32]. In this regard, depending on the dye aggregation, the photophysical properties of the material can be drastically changed. Considering the formation of dimers as the first state in the molecular aggregation process, there are two main types: case A) perfect H-dimers (monomers disposed in parallel planes in a sandwich-like conformation) are characterized by new absorption bands at lower wavelength respect to the monomer band and case B) perfect J-dimers (monomers in line in a head-to-tail disposition) show absorption bands at higher wavelength respect to monomer band (Scheme 2). Besides, dimers can usually adopt structures with intermediate geometries to optimize the attractive permanent/induced/instantaneous dipole interactions and to minimize the repulsive interactions and steric hindrances between monomeric units. In these cases, dimers can show both absorption bands (blue- and red-shifted respect to the monomer band) being the H-band more intense for a twisted sandwich-type dimer (case D1, Scheme2), whereas the J-band will be more intense in an oblique head-to-tail dimer (case D2, Scheme 2). Indeed, Fujii et al.[33] have proposed a ratio between the absorption intensities (obtained from the area under the curve) of both H- and J-bands as an indicative parameter for the dimer geometry: A_H/A_J values of ≥ 1.3 and ≤ 0.7 indicative of a twisted sandwich and an oblique head-to-tail geometry, respectively. Regarding their fluorescence properties, H-aggregates are not fluorescent and also dramatically quench the fluorescence of the monomer units, decreasing enormously the fluorescence lifetime and quantum yield of the system. However, J-aggregates can be potentially fluorescence although their relative quantum yield would be smaller than that of the monomers[34]. Indeed, red-emission from J-aggregates of PY dye have already detected in different 1D-channelled systems[35–39].

Scheme 2. Exciton splitting of the electronic excited states of dimers with different geometries. (radiative deactivation: continuous arrows, and non-radiative deactivation: dashed arrows).

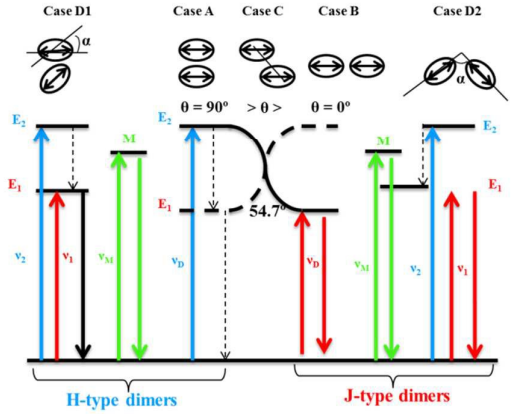

In this study, the type and extent of the aggregation of PY intercalated into two different smectite clay films is deeply analyzed. By means of evolution of the absorption spectra of PY/clay films with the dye loading, the association constant and the spectra of the dimer are calculated at moderate dye concentrations. The experimental results are confirmed theoretically by modelling the distribution of the dye into the interlayer space of the clay minerals. On the other hand, the photoluminescence of the PY/clay films as the concentration increase is also studied by steady state fluorescent spectroscopy. With the aim of minimizing the molecular aggregation of PY dye into the interlayer space of the clay film and consequently increasing the fluorescence efficiency of the system, a surfactant, dodecyltrimethylammonium bromide (DDTAB), is co-intercalated together with the dye. In this sense, it is well documented that the co-intercalation of surfactant molecules in the interlayer space of the clays minerals can reduce the dye molecular aggregation and/or change their state, i.e. from the undesirable H-aggregates to potential fluorescent J-aggregates [40–42].

Finally, the orientation of dye molecules respect to the normal axis of the clay layer is also determined in all dye/clay films by means of the anisotropic response to the plane of the polarized light in order to complete the characterization of the hybrid material[11,12,14,15,43,44].

EXPERIMENTAL AND COMPUTATIONAL METHODS

Materials

The laponite (Lap) a synthetic hectorite clay mineral in its Na^+ form with a cation exchange capacity (CEC) of 73.3 meq/100g and small particle size (disk-like particles of around 1 nm thickness and 25 nm diameter) was supplied by Laporte Industries Ltd. Saponite clay mineral (Sap), with a CEC of 56.8 meq/100g was supplied by the Clay Minerals Society (Boulder, CO) and was used in its Na^+ form and particle size lower than 0.2 µm (previously obtained as described elsewhere)[45]. Laser

This journal is © The Royal Society of Chemistry 20xx

Physical Chemistry Chemical Physics Accepted Manuscript

Please do not adjust margins

grade pyronin Y dye (PY) purchased from Exciton and surfactant dodecyltrimethylammonium bromide (DDTAB) supplied by Sigma Aldrich (purity > 99%), were used without further purification.

Dye/clay films

Supported thin solid films of both clay minerals were prepared by the spin-coating technique (BLE spinner, model Delta 10). Few drops of a well-dispersed 1.5% and 2% w/w suspension in water of Lap and Sap, respectively, were extended on a glass plate. The clay films were obtained after two consecutive spinning steps: the first at 500 rpm during 30 s and the second at 2500 rpm during 60 s. After the spinning process, the clay films were dried in an oven at 60˚C overnight. The incorporation of dye molecules into clay films was conducted by the immersion of the films in PY aqueous/ethanol solution (v/v of 50/50%). The dye loading was modified changing the immersion time (from minutes up to days) and the concentration of the dye solution (10^{-5} - 10^{-4} M). After the adsorption of the dye, the films were rinsed three times with ethanol (Merk, Uvasol) and once with water, and dried in an oven at 40˚C overnight.

The surfactant DDTAB is absorbed into the interlayer space of the clay mineral previously to the dye intercalation process by the immersion of Lap films into the CTBA solution of concentration between 10^{-6} M and 10^{-5} M from some minutes to hours.

Instrumental

The interlayer space of the dye-clay films was determined by X-ray diffraction (Philips, model PW 1710). The amount of organic molecules incorporated (dye and surfactant) is estimated by elemental analysis (Euro EA 3000 series Elemental Analyser). Thermogravimetric analysis TGA (Mettler Toledo TGA/SDTA 851E) was used to estimate the water content. The thickness of the films is obtained by optical profilometry (Alpha-step D100) at the centre of the films, Absorption and fluorescence spectra of PY/clay films were recorded by means of an UV/Vis spectrophotometer (Varian, model CARY 4E) and a fluorimeter (SPEX, model Fluorolog 3-22). All absorption spectra were registered in the transmittance mode. The dispersion of the incident light by the clay films was corrected by placing a clay film without dye in the reference beam. The emission spectra were recorded in the front face mode by detecting the emitted light at 22.5˚ with respect to the incident beam.

Absorption spectra with linearly polarized light were recorded using a Glam-Thompson polarizer in the incident (absorption) beams. The anisotropy study was performed by recording the absorption spectra for horizontal (X-axis, A_X) and vertical (Y-axis, A_Y) polarized light with respect to the incident beam (Z-axis) for different orientations of the sample with respect to the incident light, by twisting the supported film around its Y-axis at different δ angles, as is described in ref[10]. The dichroic ratio ($D_{X,Y}$), obtained from the relation between both spectra ($D_{X,Y} = A_X/A_Y$), was evaluated for δ angles from 0˚ up to 70˚. The intrinsic responses of the optical components of the spectrophotometer were corrected by recording the dichroic response of the instrument of an isotropy sample (PY solution 10^{-5} M in a 1 mm cuvette) at every scanned δ angle.

Computational Simulations

Laponite and saponite were built by modifying their natural analogues described by Breu et al[46] and Rayner[47] respectively, following similar procedures as shown in ref[48]. The necessary number of water and dye molecules to achieve experimental composition was randomly incorporated to the interlaminar spaces[49]. The relaxed structure of the dye and its atomic charges within the ChelpG Scheme[50] were determined by density functional theory (DFT) simulations using the Gaussian09 code[51], with a 6-3111+G(d,p) basis set and the exchange correlation functional B3LYP[52].

LAMMPS simulation package[53] were used to carry out the molecular dynamics (MD) simulations. ClayFF[54] and CHARMM[55] force fields were used to describe the bonding and VdW interactions in clays and dyes respectively, while the electrostatic forces were evaluated by the pppm method[56], using the charges defined by ClayFF for the clays and those obtained from DFT simulations for the dyes.

The energy of the hybrid systems was minimized relaxing both the box parameters and the atomic positions. Afterwards, molecular dynamics in the canonical ensemble (NVT) was performed at 300K during 250 ps. It was used a thermostat coupling constant of 0.1 ps and a time step of 1fs, using Verlet algorithm[57] for the integration of the equations of motion. Then, we equilibrated the atomic positions and volume under room conditions (300K and 1 atm) turning to the isobaric-isothermal ensemble (NPT) during 1 ns. Finally, a canonical ensemble was carried out during 0.1 μs to average the system properties.

RESULTS AND DISCUSSION

Transparent films of clay, adequate for dye adsorption were made by spin coating and the thickness of the supported thin-films was checked by Laser profilometry. The thickness of Lap films of around ~ 400 nm is higher than in Sap of ~ 100 nm (Figure 1), due to the very stable and viscous aqueous suspensions obtained for Lap as a consequence of its small particle size (~25 nm) respect to saponite (≤ 200 nm).

Nevertheless, the thickness of the Sap films is thick enough to allow a proper photophysical characterization of the films[58]. After the dye intercalation process, instead of the total amount of dye, we considered the percentage of the cationic exchange capacity of each clay mineral occupied by PY cations (% CEC) as the most representative parameter for the comparison between both clay films. In this sense, by increasing the immersion time of the pure clay films into PY dye solution of 10^{-5} M from few minutes to several hours, an increase in the % CEC from 0.5% to 10% is reached in Lap films (5 min - 8h) and from 0.9 to 20% in Sap films (15 min - 49h)

Physical Chemistry Chemical Physics Accepted Manuscript

(Table 1). Longer immersion times into 10^{-5} M PY solution do not produce significant increase in the % CEC (Figure 1) due to the equilibrium concentration is established between the films and the dye solution. To reach further increase in the % CEC, the clay films were immersed in a more concentrated dye solution (10^{-4} M) varying the time from hours to days, up to reach dye saturated films with similar % CEC values of 27% and 32% for Lap and Sap films, respectively (Table 1).

X ray diffraction technique was used to confirm the incorporation of PY dye molecules in the interlayer space[58]. According to the XRD patterns, as the dye loading increase the 001 peak of the clay films shifts to lower 2θ values (Figure 2), indicative of the swelling of the interlayer space of the clay mineral by the presence of PY molecules. However, there are significant differences in the evolution of 001 peak with the dye loading between both clay films. In the case of Lap, the interlayer space increases gradually with the dye uptake and with a more pronounced swelling at moderate dye loading (≤ 20% CEC) than in Sap films (Table 1). This result could be attributed to: i) the localization of the net negative charge of the clay minerals, i.e. the isomorphous substitution at external surface (tetrahedral layer) in Sap can reduce its swelling capacity respect to the Lap sited at the internal octahedral layers, as other authors have described[59]; and/or ii) to the different molecular association (aggregates), distribution and orientation adopted by dye molecules in the interlayer space of each clay, although other factors such as the differences in their CEC and particle size could also influenced. According to previous studies[10], the progressive increase of the interlayer distance could denote a more perpendicular orientation of the PY molecules respect to the clay surface as the dye content increased. Note here that the basal space obtained by XRD is an average value for all the interlayer distances, which is usually underestimated for films with low-moderate dye loadings because not all the interlayer spaces are equally swelled[59].

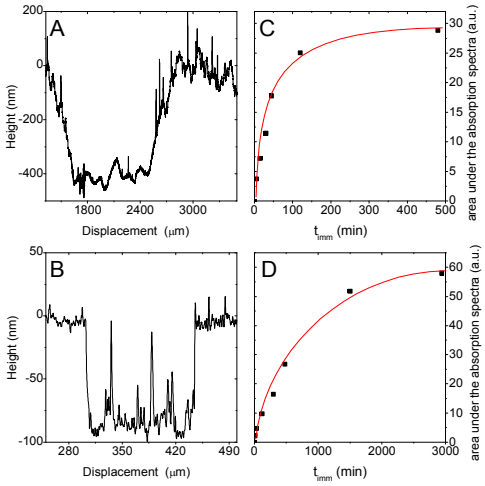

Figure 1. Thickness measured by optical profilometry of Lap (A) and Sap (B) films at the center of the film. Dye loading in the interlayer space estimated by the area under the absorption spectra as a function of the immersion time into 10^{-5} M PY solution in Lap (C) and Sap (D) films.

Table 1. Data of PY/Sap (S), PY/Lap (L) and PY/Lap with previous DDTAB absorbed (L^{+su}) films at different dye loadings: time (immersion time of clay films into PY 10^{-5} M solution); d_{001} (Interlayer space distances of PY clay films); λ_{abs} (absorption wavelength); λ_{flu} (fluorescence wavelength); E_{flu} (fluorescence efficiency determined from the area under the emission curve and the absorbance of the sample at the excitation wavelength), ψ (tilted angle between the long molecular axis of PY dye and the normal to the clay layer obtained from absorption with polarized light).

% CEC	Time (h)	d_{001}	λ_{abs} (nm)	λ_{flu} (nm)	E_{flu} ($x10^{-8}$)	ψ
0.5 L	0.1	12.9	547	563	11	-
1.1 L	0.25	-	541	565	6.6	-
0.9 S	0.25	12.5	554	563	17	-
1.8 L	0.5	-	547/471	566	0.53	63
2.5 L	0.75	13.4	544/473	566	0.26	62
1.7 S	0.5	12.5	554	564	9.1	62
$2.4L^{+su}$	0.75	13.8	553	568	10	62
3.8 L	2	-	541/471	568	0.12	-
3.7 S	2	-	555	566	3.9	-
4.5 L	4	14.8	536/468	566/672	0.04	61
6.6 S	5	12.5	557	570	1.8	61
10.2 L	8	15.2	473	682	0.03	62
10.0 S	8	12.5	557	572	1.2	61
$9.3L^{+su}$	8	15.5	541/474	572/665	3.8	61
20 S	16	12.6	558	574/614/670	8.2	61
15 L	2*	15.6	489	685	0.025	59
22 S	49	13.0	560/516	574/616/675	0.2	60
27 L	24*	15.7	492	687	0.02	58
32 S	24*	13.4-15.8	508	575/628/678	0.04	58

*immersion of clay film into PY solution of 10^{-4} M

However, for very high dye loading, the estimation of the orientation of dye molecules by the interlayer distance is usually more accurate. Indeed, at saturated dye conditions similar increase of the interlayer space, around 15.8 Å, are obtained in both clay films (Table 1, Figure 2). Assuming that the interlayer space is given by the projection of the long-molecular axis of PY (13.2Å) to the c-axis, the tilted angle obtained between the long-molecular axis and the normal to the surface for dye saturated films of both clays is around 62˚, denoting a relatively planar distribution of the PY molecules. Nevertheless, a more detailed study on the orientation of dye molecules adsorbed in clay films at different loading will be described later in this work by means of UV-Vis absorption spectroscopy with linear polarized light. On the other hand, it is important to note also here that in the diffractogram of the saturated Sap film (32% CEC) also show another overlapped peak at higher angles (Figure 2B), indicative of an inhomogeneous covering of the interlayer space by dye cations, likely assigned to the lower swellability and more restricted space in Sap, above mentioned.

Physical Chemistry Chemical Physics Accepted Manuscript

This journal is © The Royal Society of Chemistry 20xx

Please do not adjust margins

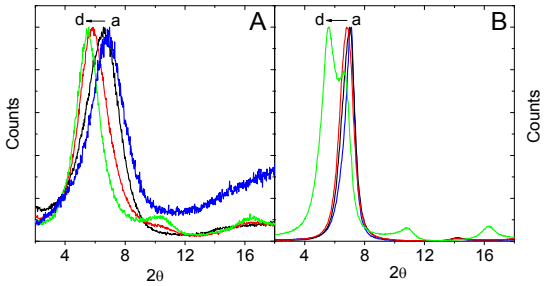

Figure 2. Normalized X-ray diffractions of PY at different dye loadings (in % CEC): (A) laponite; pure Lap (a), 2.5% CEC (b), 10.2% CEC (c), 27% CEC (d) and (B) saponite; pure Sap (a), 1.8% CEC (b), 20% CEC (c), 32% CEC (d).

The increase of PY loading not only produces an intensification of the global color of the films but also a change in the tonality, modifying the shape of the absorption spectra (Figure 3) in both clay films. These changes, consisting in the replacement of the main absorption band by other absorption bands placed at lower wavelength, are known as metachromatic effect and are ascribed to the aggregation of the dye [26].

The changes in the absorption spectra with the PY dye loading are drastically different depending of the clay mineral type. For instance, in PY/Lap films very abrupt changes are registered even at very low dye content (≤ 4.5% CEC). Only, the narrow absorption band at 547 nm registered in the most diluted PY/Lap films of 0.5% CEC, is similar to that recorded in diluted aqueous solution (Figure S1), and is assigned to the monomer of PY into the interlayer space of Lap films. As the dye loading increase, the relative intensity of the main absorbance band significantly decrease and a new band centred at around 470 nm becomes apparent already at 1.1% CEC

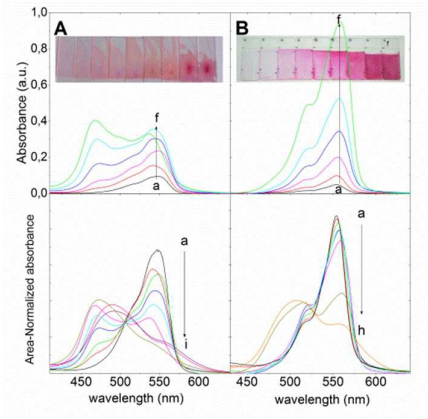

Figure 3. (top) Absorption spectra of PY and (bottom) area-normalized absorption spectra of PY (at different % CEC) into A) laponite at: 0.5% CEC (a), 1.1% CEC (b), 1.8% CEC (c), 2.5% CEC (d), 3.8% CEC (e), 4.5% CEC (f), 10.2% CEC (g), 15% CEC (h), 27% CEC (i) and into B) Saponite at 0.9% CEC (a), 1.7% CEC (b), 3.7% CEC (c), 6.6% CEC (d), 10% CEC (e), 20% CEC (f), 22% CEC (g), 31% CEC (h) (Inset picture of the corresponding dye/clay films).

The appearance of new absorption band at higher energies in detriment of the monomer band would correspond to the absorption of the H-band of a sandwich-like aggregate, likely a dimer at such low dye coverage. Actually, at 4.5% CEC of PY into Lap films, the more energetic band is already more intense than the absorption band assigned to the PY monomer. These results obtained for quite low dye content in Lap films (< 5%) indicate a high molecular aggregation process of PY dye into Lap films. In fact, for dye loading % CEC > 10%, reached by the immersion of Lap film into a more concentrated dye solution (10^{-4} M), the absorption band of the monomer practically disappears and only the more energetic band centered at around 470 nm is recorded.

Conversely, very slight changes are registered in the absorption spectra for PY into Sap films with the dye loading up to 20% CEC (Figure 3), indicating a much lower aggregation tendency of PY dye into Sap. First note that the absorption band registered in the most diluted PY/Sap film (0.9% CEC), assigned to the PY monomer absorbed in the interlayer space of Sap films, is even narrower than that obtained in aqueous solutions (Figure S1). In addition, this absorption band, placed at 554 nm, is red-shifted respect to PY in solution (547 nm), possibly as a consequence of higher dye-clay interactions in the interlayer space of Sap respect to Lap. As the dye loading increase in Sap films up to 20% CEC, the main absorption band slightly shifts to lower energies and the shoulder at higher energies at around 520 nm slightly increases with respect to the main absorption band (Figure 3). These slight changes indicate the formation of molecular aggregates, probably dimers, but in much less extent than in Lap films at similar dye concentrations. However, much evident changes are also registered for CEC > 20% (Figure 4) in PY/Sap films, i.e. absorption spectra is much wider and the adsorption band at higher energies becomes more important than the monomer band, similar tendency to that recorded in PY/Lap films at % CEC ≥10%, indicative of the formation of high-order aggregates.

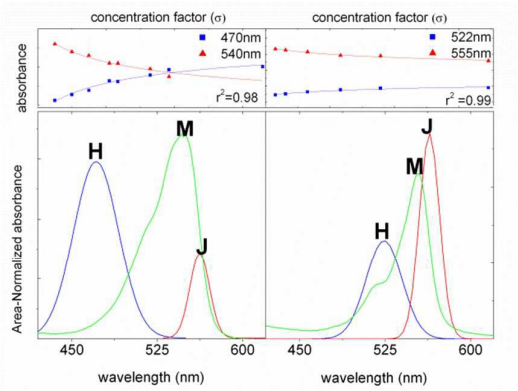

Figure 4. The monomer absorption spectra and the deconvoluted absorption bands of the dimer spectra calculated from the non-linear least square fitting process (the non-linear curve fit in each clay system at the two representative wavelengths is included) in laponite (left) and saponite (right) clays.

Physical Chemistry Chemical Physics Accepted Manuscript

To get further information about the extent and type of PY aggregates in the different clay films, the dimerization constants, K_D, and the dimer absorption spectra, ε_D (λ), are calculated in each clay films from the evolution of the concentration-normalized absorption spectra at moderated dye loadings (≤ 20% CEC) with the concentration factor, by means of a non-linear least square fitting equation obtained from the mass-law, described elsewhere[60]. The fit proposes those K_D and ε_D (λ) values that minimize the reduced chi-square between the experimental and the fitted data (detailed description in ESI)

Figure 4 shows the fit curve obtained for the PY/Lap and PY/Sap films in moderate dye loadings at the two most representative wavelengths: the main absorption band of the monomer (545 nm and 555 nm for PY/Lap and PY/Sap films, respectively); and at the absorption wavelength of the new hypsochromic band as the dye loading increase (470 nm and 522 nm for PY/Lap and PY/Sap films, respectively). The fit was done as a global analysis where K_D is an adjustable parameter but linked to be a common value to the two analysis wavelengths. All fits supply analogous values with correlation coefficients (r) close to unity, suggesting the viability of the mathematical procedure. The global analysis provides a K_D value of 0.025 for PY/Lap film (respect to an standard concentration, co ≡ 0.5% CEC) and K_D value of 0.015 for PY/Sap films (respect to an standard concentration, co ≡ 0.9% CEC) for moderate PY loading samples (≤ 10.2% CEC for PY/Lap and ≤ 20% CEC for PY/Sap films). This result clearly confirms the higher aggregation tendency of the PY molecules absorbed into the Lap films respect to the Sap films.

Once determined the K_D, the dimer spectra can be calculated for each system. In both clay films, these spectra consist in two absorption bands placed at both sides of the monomer absorption band (Figure 4). However, there are important differences in the dimer spectra of PY into both clay minerals: the H-band in PY/Lap films, placed at 471 nm, is more intense with an area under the curve around 5 times higher than that obtained for the red shifted J-band, centered at 562 nm. In contrast, the J-band placed at 564 nm obtained in PY/Sap films is slightly more intense with an area under the curve around 1.2 times higher than its H-band centered at 522 nm. According to the Exciton Theory, the geometry of the PY dimer is consistent with the twisted sandwich type (case D1 in Schema 2) in Lap films whereas an oblique head-to-tail type (case D2, Schema 2) is propoused for Sap films.

Figure 5 shows dimer geometry probability by means of combined distribution function of the angles α and θ, defined by the Exciton theory[61] (Scheme 2). The angle θ is defined by the transition dipole moment vector of one PY molecule and a vector between the center of mass of two PY molecules. On the other hand, the angle α was formed by the transition dipole moment vectors of two PY molecules.

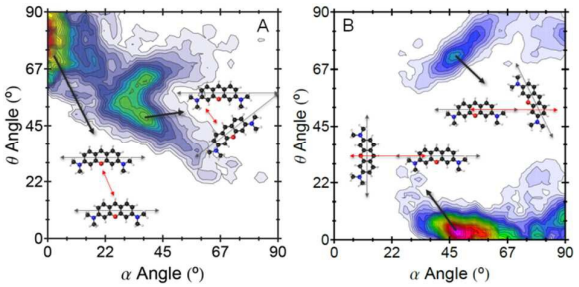

Figure 5. Angle α and θ combined distribution function of dimeric species in laponite (A) and saponite (B). The angles α and θ are both defined by Exciton theory[61] (Scheme 2).

The differences found in the extent and type of the aggregation of PY dye could be attributed to the negative charge location in the Lap and Sap, although other factors such the differences on their CEC and particle size cannot be discarded. The net negative charge at the external T-layer in Sap films allows stronger electrostatic clay/dye interactions than in Lap with an internal distribution of the negative charge in its O layer. Accordingly, dye/dye interactions are more favored in Lap films promoting high extent in the molecular aggregation in sandwich like, since this configuration maximizes the contact area between the dye molecules, which also counteract the intrinsic hydrophilic environment of the interlayer space of the clay minerals. Another important factor would be referred to the interlaminar water distribution which could influence dye aggregation. That is, the water bilayer distribution founded in the interlayer space of laponite (Figure S2) may lead to dye aggregation to minimize the solvation due to the intrinsic hydrophobic character of the organic molecule avoiding to be surrounded by water molecules. Contrary, in a water monolayer distribution, as in saponite, the water-dye interactions are less important, and the chemical driving force for aggregation is lower.

The dye aggregation tendency of PY in clay films was confirmed by fluorescence. The fluorescence efficiency of PY in each clay minerals (determined from the ratio between the area under the curve and the absorbance of the sample at the excitation wavelength, I_{flu}/A_{exc}) significantly drop in PY/Lap at even very low dye concentration (Figure 6A), i.e. the emission efficiency of a PY/Lap film of 3.8% CEC decreases around 90 times respect to the most diluted PY/Lap film of 0.5% CEC (Table 1). The loss is even more prominent at moderate dye loading with a decrease of 830 times for a PY/Lap film of 10% CEC, as a consequence of a mayor contribution of the efficient fluorescence quenchers H-type aggregates. Indeed, the emission spectra of PY/Lap films recorded for low-moderate dye loading (< 10% CEC) do not show any new bands (Figure 6A) but narrow emission bands similar to the spectra of the PY in diluted aqueous solution (Figure S1), assigned to the PY monomer emission band into Lap films. This band gradually shifts to the red as the dye loading increase (from 563 nm up to ~574 nm, Table 1) likely due to reabsorption-reemission phenomena, typical effect in optically dense materials.

Physical Chemistry Chemical Physics Accepted Manuscript

This journal is © The Royal Society of Chemistry 20xx

Please do not adjust margins

Conversely, the loss in the fluorescence for PY/Sap films as the dye loading increase is much less prominent for such moderate dye loadings, i.e. a decrease of around 4 times for a PY/Sap film of 3.7% CEC and around 14 times for a PY/Sap film of 10% CEC, with respect to the most diluted PY/Sap film of 0.9% CEC (Table 1, Figure 6B). Note here that in PY/Sap films at moderated concentration (≤ 20% CEC) new fluorescence shoulders at around 620 and 675 nm (Figure 6B, highlight with grey circle area) are weakly manifested which become evident at ≥ 22% CEC (Figure 6 inset), attributed to the fluorescence bands of J-aggregates. In the end, PY show similar reminiscent red-shifted emission in both clay films at saturated dye conditions, i.e. centered at ~675 nm in Sap for loading > 20% CEC and at ~685 nm in Lap for ≥ 10% CEC, which could be attributed to the emission of J-bands of high-ordered aggregates.

In order to reduce the dye aggregation and consequently ameliorate the drastic quenching in fluorescence observed particularly in Lap films as the dye loading increase, the surfactant dodecyltrimethylamonium (DDTAB) is co-intercalated together with the dye. It is well known that the co-adsorption of surfactant can counteract the hydrophilic environment of the interlayer space of the clay mineral reducing the organic dye molecular aggregation[40,42,62]. For that propose two representative PY/Lap films with a dye loading of 2.5% and 10.2% CEC are chosen to be synthesized with surfactant co-intercalated. Thus, the surfactant is intercalated by the immersion of Lap film into the DDTAB solution previously to the dye intercalation process. Several experiments with different amounts of surfactant adsorbed (by varying the immersion time and concentration of DDTAB solution) have been carried out with the aim of optimized the photophysical properties of PY/Lap films. Then, the dried surfactant/Lap films were immersed into 10^{-5} M PY solution at the corresponding immersion times set at 45 min and 8h for the Lap films with PY loading of 2.5% CEC and 10.2% CEC, respectively. The final amount of intercalated PY dye in the film with surfactant was estimated photometrically by the area under the resultant absorption curve.

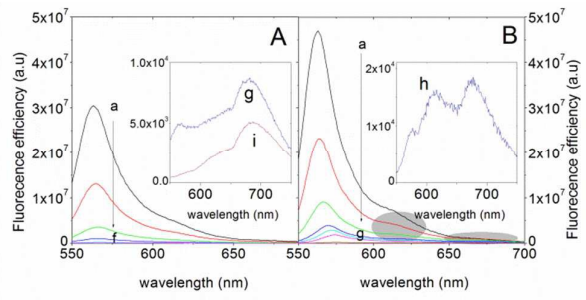

Figure 6. Fluorescence efficiency of PY films with different dye loadings (in % CEC): (A) PY/Lap films of 0.5% CEC (a), 1.1% CEC (b), 1.8% CEC (c), 2.5% CEC (d), 3.8% CEC (e), 4.5% CEC (f), 10.2% CEC (g), 15% CEC (h), 27% CEC (i) and (B) PY/Sap films of 0.9% CEC (a), 1.7% CEC (b), 3.7% CEC (c), 6.6% CEC (d), 10% CEC (e), 20% CEC (f), 22% CEC (g), 31% CEC (h).

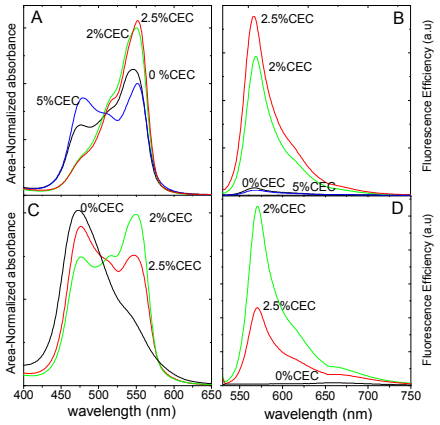

Figure 7. (A, B) Absorbance spectra and (B, D) fluorescence efficiency of PY/Lap films of (top) 2.4% and (bottom) 9.3% CEC dye loading with 0% CEC, 2% CEC, 2.5% CEC, and 5% CEC of surfactant previously adsorbed in Lap thin film obtained by immersion of the pure lap film into DDTAB 50/50 (v/v) water/EtOH solution 10^{-6} M during 2h and 6 h and into 10^{-5} M during 1 h, respectively.

In fact, the presence of the surfactant in the interlayer space does not practically modify the interlayer space of the pure Lap films (Figure S3 and Table S1) neither the total amount of the dye adsorbed with respect to the PY/Lap films without surfactant, reaching similar CEC of 2.4% and 9.3% for 45 min and 8 h immersion times, respectively (Table 1). However, important changes in the shape absorption spectra are registered in both samples (Figure 7). In the PY/Lap film of 2.4% CEC, the absorption band centered at higher energies, around 470 nm, previously assigned to H-band of aggregates, nearly disappears and the monomer band at 550 nm is only recorded for a surfactant concentration between 2-2.5% CEC previously intercalated. This fact indicates that an important dye disaggregation process takes place in presence of an appropriate amount of surfactant. Note here that CEC > 2.5% of surfactant incorporated into Lap films (i.e. 5% CEC) leads to a higher molecular aggregation (Figure 7A), whereas CEC < 2% does not practically modify the aggregation state of PY into Lap films (data not-shown). Likewise, very significant disaggregation process can be also reached for the sample with 9.2% CEC of dye by the presence of the surfactant in the interlayer space. The only absorption band at around 470 nm previously recorded for 10.2% CEC PY/Lap film without surfactant ascribed to H-aggregates, is significantly decreased in detriment of the PY monomer band at 547 nm for the homologous PY/Lap film of 9.2% CEC with a surfactant loading between 2-2.5% CEC (Figure 7B). Indeed, the monomer band is registered as the main absorption band at a surfactant concentration of 2% CEC, indicating that a higher molecular disaggregation has been reached with respect to a surfactant amount of 2.5% CEC. Although seems that in this case the optimized surfactant concentration is in a very narrow range (2-2.5% CEC), it can be easily controlled by the immersion of pure Lap films into diluted DDTAB solution of 10^{-6} M and varying the immersion times between 2h and 6h, for 2% and 2.5% of CEC, respectively. In fact, although similar results could

Physical Chemistry Chemical Physics Accepted Manuscript

be reached carrying out the intercalation of the surfactant and dye simultaneously, by immersion of pure Lap films into PY/DDTAB solutions of different concentration ratio (Figure S4), is very difficult to control the optimal amount of surfactant and this methodology and is not recommended.

The disaggregation tendency of PY dye molecules by the presence of surfactant molecules in the interlayer space of Lap at the optimized DDTAB concentration is nicely confirmed by the fluorescence properties of the films (Figure 7C,D). Indeed, the fluorescence efficiency for a PY/Lap films of 2.4% CEC of dye and 2.5% CEC of surfactant has increased at around 40 times respect to the equivalent PY/Lap sample without surfactant (Table 1), practically recovering the fluorescence capacity registered for the PY into the most-diluted Lap films of 0.5% CEC (Table 1). Moreover, much impressive improvement is reached in the fluorescence properties of the PY/Lap film with 9.3% CEC of dye intercalated and 2% CEC of surfactant co-absorbed with respect to homologous PY/Lap film of 10.2% CEC dye loading without surfactant. In this case, the reminiscent band centered at 682 nm, previously assigned to the emission of J-band of high-order aggregates, revert to the monomer emission band at around 570 nm with fluorescence efficiency 100 times greater. The less increase of the emission, of around 45 times, obtained for a surfactant loading of 2.5% CEC respect to 2% CEC (Figure 7D) is in accordance with the changes also seen in the visible spectra (Figure 7C) indicating a lower disaggregation process at that surfactant amount.

Finally, similar orientation angles of PY molecules respect to the normal to the clay film, evaluated by UV-Vis absorption spectroscopy with linear polarized light (Table 1, Figure 4, S5, S6, S7 and S8), are obtained for the most representative dye/clay films (with and without surfactant), (Table 1). Generally, PY molecules adopt a relative parallel disposition to the clay layer with a tilted angle of around 62-63˚ with respect to the film normal for low and moderated dye loading that slightly varies to 58˚ at saturated dye films. This titled angle derived from the experiments with linear polarized light agrees well with the previously estimated by XRD at high dye loading (62°). More importantly, it is confirmed a macroscopic order in all these dye/clay films indicating that the co-adsorption of surfactant molecules do not disrupt the orientation of the PY dye molecules (Figure S7 and S8) in the interlayer space of the clay films.

Conclusions

According to the experimental and theoretical results, different types and extents of the aggregation of PY dye molecules take place in Lap with respect Sap clay films. The reason is attributed to the different strength of electrostatic interactions between the dye and the clay mineral and the different water distribution in the interlayer space of both clay minerals. The net negative charge at the external T-layer in Sap films allows stronger electrostatic clay/dye interactions than in Lap with an internal distribution of the negative charge in its O layer. Accordingly, a better dye distribution is achieved in interlayer space of Sap reducing the molecular aggregation and favouring J-type aggregates, a more open geometry in which the dye molecules are in better contact with the clay surface. On the contrary, the water bilayer distribution founded in the interlayer space of laponite and the less effective dye-clay interactions lead to a higher dye aggregation in H-type geometry to maximize the contact area between the dye molecules counteracting the hydrophilic environment of the interlayer space. By co-intercalation surfactant molecules in the Lap interlayer space at an optimized concentration, the aggregation process is diminished and the fluorescence properties have been significantly improved.

Finally, all the films analyzed showed anisotropic response to the linear polarized light indicating a regular orientation of adsorbed PY dye molecules towards the normal to the clay film. They adopt a relative parallel disposition to the clay layer with a tilted angle of around 62-63˚ with respect to the film normal for low and moderated dye loading that slightly vary to 58˚ at saturated dye clay films. Importantly, the co-adsorption of surfactant molecules has improved the fluorescent properties of the hybrid films without disrupting the orientation of the PY dye molecules.

Acknowledgements

The authors thank the Spanish Ministry of Economy and Competitiveness, MINECO, (MAT 2014-51937-C3-3) and Basque Government (IT339-10 and IT912-16) for funding this research. VMM and HMM acknowledge the Ministry of Economy and Competitiveness, MINECO, for 'Ramón y Cajal' (RYC-2011-09505) and 'Juan de la Cierva' contracts. NEE and EDR acknowledge the University of Basque Country (UPV-EHU) for pre-doctoral fellowships. The authors thank for technical and human support provided by IZO-SGI SGIker of UPV/EHU, i2Basque project and European funding (ERDF and ESF).

Notes and references

1 M. Ogawa and K. Kuroda, *Chem. Rev.*, 1995, **95**, 399–438.
2 C. Sanchez, B. Julián, P. Belleville and M. Popall, *J. Mater. Chem.*, 2005, **15**, 3559–3592.
3 L. Cerdán, A. Costela, I. García-Moreno, J. Bañuelos and I. López-Arbeloa, *Laser Phys. Lett.*, 2012, **433**, 426–433.
4 J. Gong, J. Liang and K. Sumathy, *Renew. Sustain. Energy Rev.*, 2012, **16**, 5848–5860.
5 G. Schulz-Ekloff, D. Wöhrle, B. van Duffel and R. A. Schoonheydt, *Microporous Mesoporous Mater.*, 2002, **51**, 91–138.
6 R. H. A. Ras, Y. Umemura, C. T. Johnston, A. Yamagishi and R. A. Schoonheydt, *Phys. Chem. Chem. Phys.*, 2007, **9**, 918–932.
7 P. Innocenzi and B. Lebeau, *J. Mater. Chem.*, 2005, **15**, 3821–3831.
8 M. Ogawa, M. Sohmiya and Y. Watase, *Chem. Commun. (Camb).*, 2011, **47**, 8602–8604.
9 F. López Arbeloa, V. Martínez Martínez, T. Arbeloa and I. López Arbeloa, *J. Photochem. Photobiol. C Photochem. Rev.*, 2007, **8**, 85–108.

Physical Chemistry Chemical Physics Accepted Manuscript

This journal is © The Royal Society of Chemistry 20xx

Please do not adjust margins

10 V. Martínez-Martínez, F. López-Arbeloa, J. Bañuelos and I. López-Arbeloa, *Chem. Mater.*, 2005, **17**, 4134–4141.
11 Y. Kaneko, N. Iyi, J. Bujdak, R. Sasai and T. Fujita, *J. Colloid Interface Sci.*, 2004, **269**, 22–25.
12 M. Iwasaki, M. Kita, K. Ito, A. Kohno and K. Fukunishi, *Clays Clay Miner.*, 2000, **48**, 392–399.
13 F. López Arbeloa and V. Martínez Martínez, *Chem. Mater.*, 2006, **18**, 1407–1416.
14 S. Takagi, T. Shimada, Y. Ishida, T. Fujimura, D. Masui, H. Tachibana, M. Eguchi and H. Inoue, *Langmuir*, 2013, **29**, 2108–19.
15 N. Sato, T. Fujimura, T. Shimada, T. Tani and S. Takagi, *Tetrahedron Lett.*, 2015, **56**, 2902–2905.
16 Y. Suzuki, Y. Tenma, Y. Nishioka and J. Kawamata, *Chem. - An Asian J.*, 2012, **7**, 1170–1179.
17 N. Epelde-Elezcano, E. Duque-Redondo, V. Martinez-Martinez, H. Manzano and I. López-Arbeloa, *Langmuir*, 2014, **30**, 10112–10117.
18 Y. Ishida, R. Kulasekharan, T. Shimada, V. Ramamurthy and S. Takagi, *J. Phys. Chem. C*, 2014, **118**, 10198–10203.
19 V. Ramamurthy, S. Jockusch and M. Porel, *Langmuir*, 2015, **31**, 5554–5570.
20 D. H. Volman, G. S. Hammond, D. C. Neckers, V. Ramamurthy and R. G. Weiss, *Adv. Photochem.*, 1993, **18**, 67–236.
21 S. M. Auerbach, K. a. Carrado and P. K. Dutta, *Handbook of Layered Materials*, CRC Press, 2004.
22 F. López-Arbeloa, I. López-Arbeloa and T. Arbeloa, in *Encyclopedia of Surface and Colloid Science*, CRC Press, 2002, pp. 2007–2020.
23 S. De, S. Das and A. Girigoswami, *Spectrochim. Acta - Part A Mol. Biomol. Spectrosc.*, 2005, **61**, 1821–1833.
24 D. C. Valdes-Aguiler, O., & Neckers, *Accounts Chem. Res.*, 1989, **22**, 171–177.
25 H. Wang, Q. Yang, L. Sun, S. Wang, W. Wang, C. Zhang, Y. Li, S. Xu and Y. Li, *J. Colloid Interface Sci.*, 2010, **341**, 224–231.
26 K. Meral, N. Ylmaz, M. Kaya, A. Tabak and Y. Onganer, *J. Lumin.*, 2011, **131**, 2121–2127.
27 A. Tabak, M. Kaya, N. Yilmaz, K. Meral, Y. Onganer, B. Caglar and O. Sungur, *J. Mol. Struct.*, 2014, **1059**, 271–279.
28 A. Czímerová, J. Bujdák and A. Gáplovský, *Colloids Surfaces A Physicochem. Eng. Asp.*, 2004, **243**, 89–96.
29 M. G. Neumann, in *Encyclopedia of surface and colloidal science*, ed. P. somasundaran, CRS Press, New York, 2012, pp. 389–410.
30 M. Epstein and S. Yariv, *J. Colloid Interface Sci.*, 2003, **263**, 377–385.
31 T. Endo, N. Nakada, T. Sato and M. Shimada, *J. Phys. Chem. Solids*, 1988, **49**, 1423–1428.
32 F. Lopez Arbeloa, T. Lopez Arbeloa and I. Lopez Arbeloa, *Trends Chem. Phys.*, 1996, **4**, 191–213.
33 T. Fujii, *Chem. Phys. Lett.*, 1995, **233**, 424–429.
34 A. Arques, A. M. Amat, L. Santos-Juanes, R. F. Vercher, M. L. Marín and M. a. Miranda, *J. Mol. Catal. A Chem.*, 2007, **271**, 221–226.
35 H. Lemmetyinen and E. Vuorimaa, *Society*, 1996, **3654**, 13701–13715.
36 R. García, V. Martínez-Martínez, R. Sola Llano, I. López-Arbeloa and J. Pérez-Pariente, *J. Phys. Chem. C*, 2013, **117**, 24063–24070.
37 V. Martínez-Martínez, R. García, L. Gõmez-Hortigüela, J. Pérez-Pariente and I. Lõpez-Arbeloa, *Chem. - A Eur. J.*, 2013, **19**, 9859–9865.
38 V. Martínez-Martínez, C. Corcóstegui, J. Bañuelos Prieto, L. Gartzia, S. Salleres and I. López Arbeloa, *J. Mater. Chem.*, 2011, **21**, 269–276.
39 M. Busby, C. Blum, M. Tibben, S. Fibikar, G. Calzaferri, V. Subramaniam and L. De Cola, *J. Am. Chem. Soc.*, 2008, **130**, 10970–10976.
40 S. Salleres, F. López Arbeloa, V. Martínez-Martínez, T. Arbeloa and I. López Arbeloa, *J. Phys. Chem. C*, 2009, **113**, 965–970.
41 S. Salleres, F. López Arbeloa, V. Martínez-Martínez, C. Corcóstegui and I. López Arbeloa, *Mater. Chem. Phys.*, 2009, **116**, 550–556.
42 R. Sasai, N. Iyi, T. Fujita, F. López Arbeloa and V. Martínez-Martínez, *Thin Solid Films*, 2004, **20**, 4715–4719.
43 J. Bujdák, V. Martínez-Martínez, F. López Arbeloa and N. Iyi, *Langmuir*, 2007, **23**, 1851–1859.
44 Y. Kaneko, N. Iyi, J. Bujdák, R. Sasai and T. Fujita, *J. Mater. Res.*, 2011, **18**, 2639–2643.
45 M. J. Tapia Estevez, F. Lopez Arbeloa, T. Lopez Arbeloa and I. Lopez Arbeloa, *Langmuir*, 1993, **9**, 3629–3634.
46 J. Breu, W. Seidl and A. Stoll, *Z. anorg. allg. Chem.*, 2003, **629**, 503–515.
47 J. H. Rayner, *Min. Mag.*, 1974, **39**, 850–856.
48 E. Duque-Redondo, H. Manzano, N. Epelde-Elezcano, V. Martínez-Martínez and I. López-Arbeloa, *Chem. Mater.*, 2014, **26**, 4338–4345.
49 C. Steffen, K. Thomas, U. Huniar, A. Hellweg, O. Rubner and A. Schroer, *J. Comput. Chem.*, 2010, **31**, 2967–2970.
50 C. M. Breneman and K. B. Wiberg, *J. Comput. Chem.*, 1990, **11**, 361–373.
51 M. Frisch, G. W. Trucks, H. B. Schlegel, G. E. Scuseria, M. A. Robb, J. R. Cheeseman, G. Scalmani, V. Barone, B. Mennucci and G. A. Petersson, *Inc., Wallingford, CT*, 2009, **200**.
52 K. Kim and K. D. Jordan, *J. Phys. Chem.*, 1994, **98**, 10089–10094.
53 S. Plimpton, *J. Comput. Phys.*, 1995, **117**, 1–19.
54 R. T. Cygan, J.-J. Liang and A. G. Kalinichev, *J. Phys. Chem. B*, 2004, **108**, 1255–1266.
55 B. R. Brooks, R. E. Bruccoleri, B. D. Olafson, D. J. States, S. Swaminathan and M. Karplus, *J. Comp. Chem.*, 1983, **4**, 87–217.
56 H. Grubmüller, H. Heller, A. Windemuth and K. Schulten, *Mol. Simul.*, 1991, **6**, 121–142.
57 J. V. L. Beckers, C. P. Lowe and S. W. De Leeuw, *Mol. Simul.*, 1998, **20**, 369–383.
58 V. Martínez-Martínez, F. López Arbeloa, J. Bañuelos Prieto, T. Arbeloa and I. López Arbeloa, *Langmuir*, 2004, **20**, 5709–5717.
59 T. Endo, N. Nakada, T. Sato and M. Shimada, *J. Phys. Chem. Solids*, 1989, **50**, 133–137.
60 V. Martínez-Martínez, F. López-Arbeloa, J. Bañuelos Prieto and I. López Arbeloa, *J. Phys. Chem. B*, 2005, **109**, 7443–7450.
61 M. Kasha, H. R. Rawls and M. Ashraf El-Bayoumi, *Pure Appl. Chem.*, 1965, **11**, 371–392.
62 J. Bujdák and N. Iyi, *Chem. Mater.*, 2006, **18**, 2618–2624.

Physical Chemistry Chemical Physics Accepted Manuscript